Cosmology with the Shear-Peak Statistics

Jörg P. Dietrich[1] and Jan Hartlap[2]
[1]ESO, Garching, Germany, [2]Argelander-Institut für Astronomie, Bonn, Germany

The Idea

The number density of clusters of galaxies is a sensitive probe for the total matter density of the Universe Ω_m, the normalisation of the power spectrum σ_8, and the evolution of the equation of state of the Dark Energy w. Due to shape noise and the alignment of large-scale structure (LSS) along the line-of-sight (LOS), weak-lensing searches for galaxy clusters have both low purity and completeness (e.g., Hamana et al. 2004; Dietrich et al. 2007). Galaxy clusters aligned with underdense regions are not visible as significant overdensities, while the projection of uncorrelated overdensities can mimic the shear signal of galaxy clusters.
Of course such projected peaks are noise or false positives only in the sense of galaxy cluster searches. They are caused by real structures along the line-of-sight and as such carry information about the matter distribution. Whereas analytical models exist for the halo mass function, no such model exists for the number density of peaks in weak lensing surveys. Probably no such prediction can be made analytically because the abundance of peaks depends on projections of uncollapsed yet highly non-linear structures like filaments of the cosmic web. As an additional complication, the observed number of peaks depends on observational parameters like limiting magnitude, redshift distribution, and intrinsic ellipticity dispersion.

In the absence of an analytic framework, ray-tracing through N-body simulations can be used to numerically compute the "peak function" (in analogy to the mass function) for a survey and study its variation with cosmological parameters. Here we present a large set of such simulations aimed at demonstrating the usefulness of the shear-peak statistics for constraining cosmological parameters. We consider this work to be a pilot study and limit ourselves to the variation of the peak function with Ω_m and σ_8 and its ability to break the degeneracy between these two parameters encountered in the two-point cosmic-shear correlation-function.

N-body Simulations

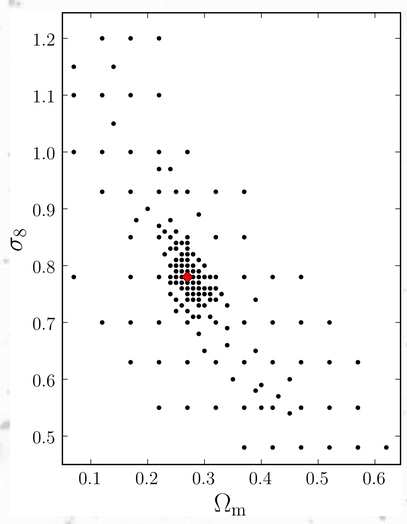

We carried out 192 N-body simulations for 158 different flat ΛCDM cosmologies with varying Ω_m, Ω_Λ, and σ_8. The figure shows the distribution of these simulations in the Ω_m-σ_8 plane. All simulations had 256^3 dark matter particles in a box with $200\,h^{-1}$ Mpc side length. With these simulation parameters we can expect the presence of $10^{15}\,h^{-1}\,M_\odot$ mass halos at redshift $z = 0$ in the simulation box in our choice of fiducial cosmology $\boldsymbol{\pi_0} = (\Omega_{m_0} = 0.27, \Omega_\Lambda = 0.73, \sigma_{8_0} = 0.78, n_s = 1.0, \Gamma = 0.21, h = 0.7)$. We did 35 N-body simulations for this fiducial cosmology to estimate the covariance of our observables. We then ray-traced through the N-body cubes to simulate a CFHTLS like survey with 180 sq. deg, consisting of 5 fields of 6×6 sq. deg. each.

Peak Tomography

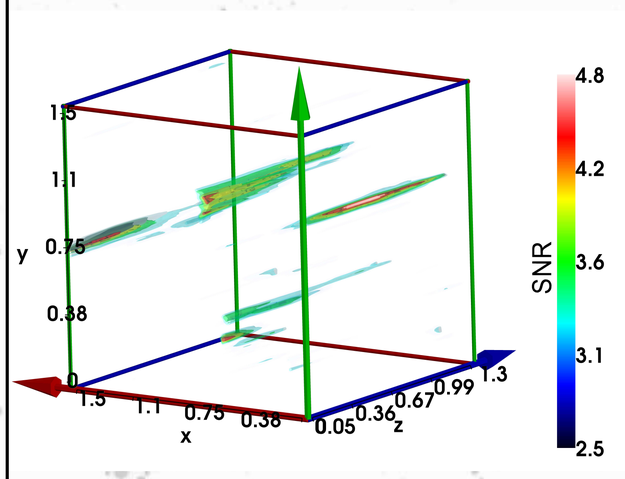

We detected peaks using the aperture-mass statistics with redshift weights (Hennawi & Spergel 2005). This tomographic matched-filter technique allows to locate peaks not only on their projected sky position but also along the redshift axis. However, because the lensing efficiency varies only very slowly with redshift, the peak tomography corresponds to smoothing along the z-axis with a very large kernel. Every structure above 3.25σ was considered as a peak.
We used the redshift distribution found in the CFHTLS-Wide survey (Benjamin et al. 2007) with a mean redshift of $\langle z \rangle = 0.802$. For this project we assumed a number density of background galaxies of $n = 25\,\mathrm{arcmin}^{-2}$ and we did not bin in redshift.

Cosmic-Shear Tomography

We measured the covariance of the cosmic-shear two-point correlation function, from the same N-body and ray-tracing simulations used for the shear-peak statistics. We divided the galaxy catalog into two redshift bins and measured the two-point auto- and cross-correlation functions

$$\xi_\pm^{(ij)}(\theta) = \langle \epsilon_t(\vartheta)\epsilon_t(\vartheta+\vartheta)\rangle \pm \langle \epsilon_\times(\vartheta)\epsilon_\times(\vartheta+\vartheta)\rangle \,,$$

at the fiducial cosmology. The cosmic-shear signal at other points in our parameter space were predicted using the non-linear power spectrum of Peacock & Dodds (1996).

Peak Statistics

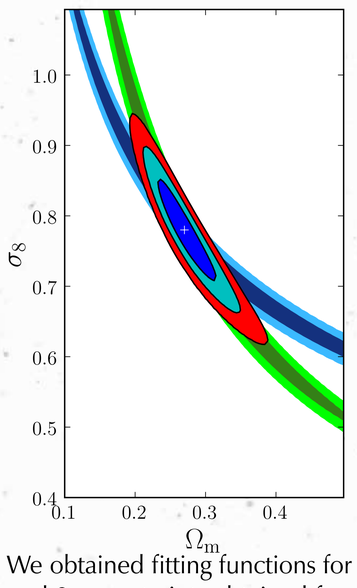

In analogy to the mass function $N(M, z)$, the peak function measures the abundance of peaks as a function of convergence and redshift $N(\kappa, z)$. Because we detected peaks not in convergence maps but in aperture-mass cubes, the SNR of peaks was used as a proxy for mass. With 175 independent ray-tracing simulations we could not compute the covariance of the full peak function $N(S, z)$ for a meaningful number of bins in SNR and redshift. Instead, we constructed two separate peak functions from the tomographic data cubes. The first function $\mathbf{M}(\boldsymbol{\pi})$ measures the abundance of peaks in 10 redshift bins $z = 0.1 \ldots 1.0$ as a function of cosmology $\boldsymbol{\pi}$ only, without dependence on SNR.
The second function uses the SNR information using the cumulative SNR distribution of peaks. The function $\mathbf{S}(\boldsymbol{\pi}) : \mathbb{R}^2 \rightarrow \mathbb{R}^m$ gives the SNR at which the cumulative distribution exceeds the fth percentile for m values of f ranging from f_{min} to f_{max}. We measured $\mathbf{S}(\boldsymbol{\pi})$ for $m = 5$ logarithmically spaced values from $f_{min} = 0.50$ to $f_{max} = 0.98$. At the fiducial cosmology these percentiles corresponds to SNR values of 3.5σ and 5.4σ, respectively.
We obtained fitting functions for $\mathbf{M}$ and $\mathbf{S}$ from our grid of N-body simulations. The figure gives the 1- and 2σ constraints obtained from $\mathbf{M}$ (green) and $\mathbf{S}$ (blue) and the 1-, 2-, and 3σ constraints from their combination including the cross-covariance between $\mathbf{M}$ and $\mathbf{S}$.

Combined Covariance

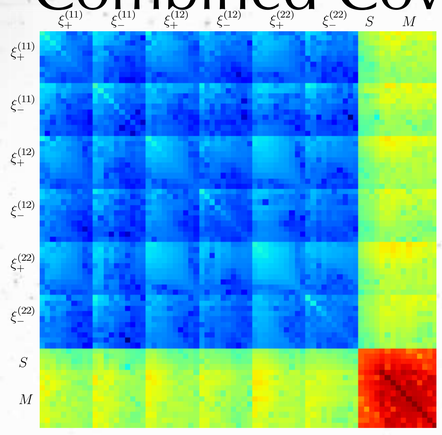

Cosmic shear and the peak statistics use the deflection of light as it passes the same LSS and thus a significant cross-covariance between the two is likely. However, the cosmic-shear 2PCF describes the underlying density fluctuations only completely if they are purely Gaussian. Cosmic shear can access information about the non-Gaussianity of the matter distribution only through higher-order correlation functions. The peak statistics on the other hand are most sensitive to extreme overdensities along the LOS, i.e., to those structures that contain the most information about non-Gaussianity.
E.g., Takada & Bridle (2007) showed that the combination of cosmic shear and cluster counts does not simply amount to counting the same information twice but can provide stronger constraints on w than either method alone. The figure shows the full covariance between the cosmic-shear tomography functions $\xi^{(ij)}$ and the peak statistics $\mathbf{M}$ and $\mathbf{S}$.

Combined Results

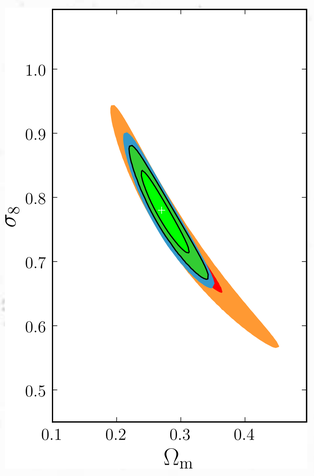

The figure on the left shows the 1- and 2σ constraints obtained from cosmic-shear tomography (orange/red), the peak statistics (blue), and the combination of both (green). The shear-peak statistics alone gives constraints on Ω_m and σ_8, which are competitive with, if not better than, those obtained from cosmic-shear tomography. However, the combination of both methods leads to little improvement as they have almost identical degeneracies.
An obvious advantage of comparing observations to ray-tracing simulations is that observational effects like, e.g., masking of bad areas, can be included in the simulations. The downside is the enormous computational cost. A Markov chain of N-body simulations is not feasible with current hardware. Population Monte Carlo methods (Wraith et al. 2009) or replacing simulations with emulations with controlled error bounds (Habib et al. 2007) should make the application of the peak statistics to existing surveys possible in the near future. We plan to extend the method to constrain Dark Energy parameters as well.

Type	Ω_m	σ_8
Peak statistics	$0.274^{+0.066}_{-0.054}$	$0.776^{+0.107}_{-0.103}$
Cosmic shear	$0.291^{+0.117}_{-0.091}$	$0.756^{+0.155}_{-0t.160}$
Combined	$0.275^{+0.057}_{-0.051}$	$0.774^{+0.095}_{-0.087}$

References

Benjamin, J., Heymans, C., Semboloni, E., et al. 2007, MNRAS, 381, 702
Dietrich, J. P., Erben, T., Lamer, G., et al. 2007, A&A, 470, 821
Habib, S., Heitmann, K., Higdon, D., Nakhleh, C., & Williams, B. 2007, Phys. Rev. D, 76, 083503
Hamana, T., Takada, M., & Yoshida, N. 2004, MNRAS, 350, 893
Hennawi, J. F. & Spergel, D. N. 2005, ApJ, 624, 59
Peacock, J. A. & Dodds, S. J. 1996, MNRAS, 280, L19
Takada, M. & Bridle, S. 2007, New Journal of Physics, 9, 446
Wraith, D., Kilbinger, M., Benabed, K., et al. 2009, arXiv:0903.0837